TRANSACTIONS OF THE INSTITUTE OF FLUID-FLOW MACHINERY

No. 124, 2012, 111–124

WITOLD ZAKRZEWSKI[a*], MICHAŁ KARCZ[a], and SEBASTIAN KORNET[a,b]

Estimation of the steam condensation flow via CFD methods

a *The Szewalski Institute of Fluid-Flow Machinery of the Polish Academy of Sciences, Centre for Thermomechanics of Fluids, Energy Conversion Department, Fiszera 14, 80-231 Gdańsk, Poland*

b *Conjoint Doctoral School at the Faculty of Mechanical Engineering, Gdansk University of Technology, Narutowicza 11/12, 80-233 Gdańsk, Poland*

Abstract

The results of numerical simulations to predict the performance of different steam models have been presented. All of the considered models of steam condensation have been validated on the base of benchmark experiment employing expansion in nozzle and next on the low pressure part of the steam turbine stage. For numerical analysis three models have been finally used – the ideal steam model without condensation, equilibrium steam model and a nonequilibrium steam model. It was confirmed that only the inclusion of the nonequilibrium effects in the computations can lead to a proper prediction of the condensation phenomena in the test nozzle. However, the basic characteristics of the low-pressure turbine can be succesfully estimated using a simple ideal steam or the equilibrium condensation model.

Keywords: Condensation model; Steam turbine; CFD

1 Introduction

Steam turbines of large output usually operate in the condensation mode. Such operation is inevitably related to phase transition phenomena occuring already in

*Corresponding Author. E-mail address:witold.zakrzewski@imp.gda.pl

the last stages of turbine low pressure part. This phenomenon was broadly investigated in the past [1, 3, 4] and for its proper description relevant mathematical models have been formulated [6, 7, 15]. However, some numerical constraints have blocked the possibility of their implementation in computational fluid dynamics (CFD).

The most unwanted effects of turbine operation at low pressure conditions are related to the spontaneous condensation. This kind of stress induced phase transition does not always occur in the vicinity of the saturation line. It can occur far from equilibrium conditions because it depends generally on the rate of pressure drop and the steam quality. In such situations the basic questions are focused on the inception and growth of water droplets due to homogenous and heterogeneous condensation [1, 3]. Process of growth of individual droplet is governed by mass, momentum and energy transport mechanism between gas and liquid phases [5, 6]. It can be described by the evolution of droplet radius.

Modelling of an inception process seems to be even more complicated. Usually, the nucleation models of von Helmholtz Jr. or Volmer and Becker-Dring are employed [3]. There is still an open question on the condensation mode occuring in the steam turbine, i.e. homogeneous or heterogeneous [10]. Usually only homogeneous condensation is being considered [11]. Several observations confirm however, that condensation often occurs earlier than it is predicted by theory, i.e., before the Wilson line [8]. It is because the nucleation can start at some soluble and insoluble impurities, particle of dust, chemical compounds or corrosion products [7]. For proper description of the heterogeonous condensation an additional model should be employed [13]. Other sources of droplets can be related to the mechanical action of steam flow on the water film that is formed at blades surface [2]. Drops created in this way are usually larger than the condensation one and are often called the secondary droplets.

Droplets of condensed phase can move with the velocity different than gas phase velocity and can seriously damage blades. Erosion of rotor blade leading edge is mainly due to droplets that form behind the trailing edge of guide vanes [4]. It is possible, using contemporary numerical tools, to model within the Lagrange-Euler framework the inception, growth and motion of such secondary droplets. This difficult issue is however omitted in the analysis.

In the present paper we have focused on the prediction of the primary condensed phase only via the Eulerian-Eulerian type of approach. The practical issue is to compare different ways of modelling of steam flow under low-pressure conditions by using an ideal steam assumption, and an equilibrium and nonequilibrium models of condensation. Model validation have been performed using experimental data for the process of steam expansion in de Laval nozzle. In the next step the flow throughout the whole low-pressure part of steam turbine has been numer-

ically analysed. For the test case the LP part equipped with Baumann stage was considered, especially due to available measurements conducted by Marcinkowski [20] and numerical investigations in 0D code Turbina by Lidke and Błażko [19]. All computations discussed in the paper have been performed using commercial CFD codes from the ANSYS package [18].

2 Condensation theory and modeling

In the equilibrium steam model the wetness is directly (algebraically) related to the pressure and the enthalpy. On the other hand the nonequilibrium model makes use of additional evolution equations. The classical analytical models of nonequilibrium production of condensed phase are usually not implementable into CFD codes [6, 7], due their noncontinual description [3], or modeling using nonlocal integral-differential evolution equations [5]. If we want to model a liquid phase evolution, we should employ a mathematical model of condensed phase production that is analogous to governing equations of mass, momentum and energy, and can be discretized using the same numerical grid.

For a consistent nonequilibrium condensation model a set of nine transport equations can be written in general form [9]

$$\partial_t (\rho\phi) + \mathrm{div}\,(\rho\phi\mathbf{v}) = \mathrm{div}\mathbf{J}_\phi + \rho S_\phi\,, \tag{1}$$

where the nine dimensional vector $\phi = \{1, \mathbf{v}, e, k, \epsilon, x, \alpha\}$ represents the relevant conserved variable. An additional balance equations for k, ϵ, x and α are related to the evolution of turbulence in the condensing flow, or the condensation evolution under turbulent flow condition. Both are fully nonequlibrium phenomena, that should be combined by the sources S_ϕ, and thermodynamical forces which constitute fluxes $\mathbf{J}_\phi$ [9]. A full phenomenological model should include the following constitutive equations for [9, 15, 16]:

- turbulent kinetic energy k:

$$\mathbf{J}_k = (D_{kk})\,\mathrm{grad}\;k + (D_{kxo} + D_{kxr})\,\mathrm{grad}\;x\,, \tag{2}$$

- dryness fraction x:

$$\mathbf{J}_x = (D_{kxo} + D_{kxr})\,\mathrm{grad}\;k + (D_{xxo} + D_{xxr})\,\mathrm{grad}\;x\,, \tag{3}$$

- turbulent kinetic energy dissipation rate ϵ:

$$\mathbf{J}_\epsilon = (D_{\epsilon\epsilon})\,\mathrm{grad}\;\epsilon + (D_{\epsilon\alpha o} + D_{\epsilon\alpha r})\,\mathrm{grad}\;\alpha\,, \tag{4}$$

- droplet number α:

$$\mathbf{J}_\alpha = (D_{\alpha\epsilon}) \operatorname{grad} \epsilon + (D_{\alpha\alpha o} + D_{\alpha\alpha r}) \operatorname{grad} \alpha \,. \tag{5}$$

Diffusion coefficients D, which are connected with homogenous related diffusion known as Ostwald mode (subscript o) and heterogeneous condensation mode (subscript r) need futher estimations and calibrations. Both these modes of condensation are present in models in an additive way and they do not influence each other. The turbulent sources can be treated in an analogical manner as the sources in the model given in [5], including turbulence production by homogenous condensation. The standard solvers however, employ models for nonequilibrium condensation that are more simplified. It is particularly related to the lack of full coupling between evolution of turbulence and spontaneous condensation.

The transport equation for x governs the nonequilibrium mass fraction of the condensed liquid phase. The dryness fraction sources S_x can be divided into homo- and heterogeneous sources of the mass generation rate due to condensation and evaporation. Homogenous source includes parts responsible for growth and inception of droplets [1, 14]

$$S_x = \frac{4}{3}\pi\rho_l I r^{*3} + 4\pi\rho_l \alpha \overline{r}^2 \dot{\overline{r}}, \tag{6}$$

where $\overline{r}$ is an average radius of droplet, ρ_l density of condensed phase, r^* is the Thomson radius, I is a volumetric rate of nucleation that can reach 10^{13} droplets/m^3 and overdot denotes the time derivative. In the framework of classical steady-state homogeneous nucleation theory the nucleation rate I takes a form [14, 10]

$$I = \frac{q_c}{(1+\nu)} \left(\frac{{\rho_v}^2}{\rho_l}\right) \left(\frac{2\sigma}{M^3\pi}\right)^{\frac{1}{2}} \exp\left(-\frac{4\pi {r^*}^2 \sigma}{3k_B T}\right), \tag{7}$$

where q_c is the evaporation coefficient, k_B is the Boltzmann's constant, M is mass of single water molecule, σ is liquid-vapour surface tension, ν is non-isothermal correction factor, and T is the temperature.

Details of nonequilibrium models are described in [5, 6, 8, 9, 10, 13]. The proper solution for steam flow under conditions close to saturation line, where non-linear dependency exists between parameters of state [17], needs a real gas equations to be employed in CFD model. These are given in a simplified form of thermodynamic state equations as virial formulations [14].

3 Numerical analysis of the de Laval nozzle

3.1 Implementation

In the present analysis the commercial code with built-in models has been employed. Three models have been considered namely: ideal steam, equilibrium condensation and nonequilibrium condensation. For the condensation models it is assumed that the droplets volume is negligibly small in comparison to the control volume, thus it is simply omitted. It is fully justified since droplet sizes are typically very small (0.1–100 μm). It is assumed also that there is no any interaction between droplets in the model and the velocity slip between the droplets and gaseous-phase is negligible. From these it follows that the mixture density, ρ, can be related to the saturated vapor density, ρ_v

$$\rho = \frac{\rho_v}{(1-x)}\,, \tag{8}$$

where x is the dryness factor.

It is assumed in the model that the mixture pressure and temperature are the same as for the vapor phase. Other assumptions are: only homogeneous condensation, spherical droplet shape, droplet is moving in the volume filled with vapor, droplet's heat capacity is negligible compared to the latent heat of condensation. The conservation equations for the liquid and gas phases are discretized and solved by means of finite volume method. A second-order upwind schemes are employed for all considered variables (Eq. 1). The turbulence stresses are modeled by means of enhanced two-equation k-ϵ model with closures Eqs. (2)–(4) in the form proposed by [9].

3.2 De Laval nozzle at Institute of Fluid-Flow Machinery

The models employed in the present analysis have been validated using an experimental data coming from supersonic flow of condensing steam throughout de Laval type nozzle installed at the Institute of Fluid-Flow Machinery PAS [1] (see Fig. 1).

A single pressure drop $p_{in}/p_{out} = 3.0$ has been chosen for numerical modelling, where p_{in} and p_{out} denotes nozzle inlet and outlet pressure, respectively. It was detected that under such conditions a shock wave forms at the nozzle exit that leads to the flow blockage. Computations have been performed for the $p_{in} = 296$ kPa, $p_{out} = 101$ kPa and inlet steam temperature $T_{in} = 180$ °C using implict coupled schemes for most of variables. Therefore simulations converge faster also in the case when the flow is simultaneously subsonic at inlet and supersonic at outlet. Less frequently used segregated solvers employ a solution strategy where the momentum equations are first solved, using a guessed pressure, and an equation for

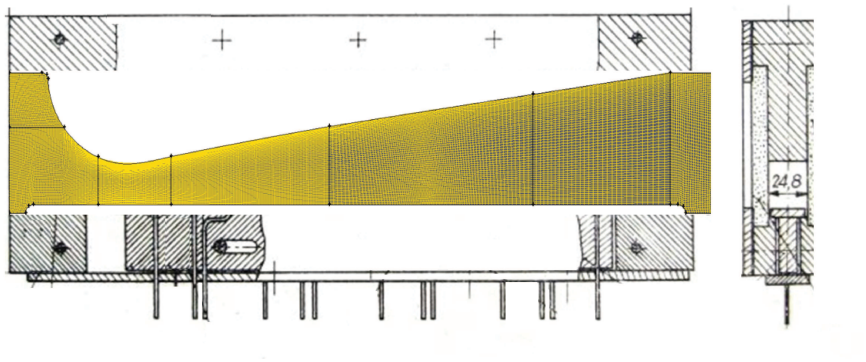

Figure 1. Discretization mesh in de Laval nozzle from IFFM PAS [1].

a pressure correction is obtained. Because of the guess-and-correct nature of the linear system, a large number of iterations are typically required in addition to the need for judiciously selecting relaxation parameters for the variables.

3.3 Validation of models

Figure 2 presents locally averaged pressure throughout the de Laval nozzle axis length. For comparison the ideal gas, the equilibrium condensation model and nine equation nonequilibrium model of wet steam are presented along the nozzle axis. Both models are validated by strict analysis of differences with experimental data taken from [1]. It should be underlined that until the condensation starts, and the thermal choking occurs, an ideal gas assumption agrees very well with the wet-steam model and experimental data. The equilibrium assumption leads to pressure overprediction at entry region however, at the nozzle exit results are predicted correctly. Generally, only nonequilibrium condensation model provides a full agreement with experiment. There is observed, however, the complex physical nature of both thermal choking conditions and shock wave flows arising under drop pressure $p_{in}/p_{out} = 3$. These internal processes influence one another in different ways, therefore there is no direct relationship between these phenomena.

3.4 Nonequilibrium effects

The local changes of static temperature are presented in Fig. 5. It can be observed that the temperature decreases when the steam is expanding. At some distance from the nozzle inlet the nonequilibrium model predicts steam subcooling below the saturation temperature estimated with the equilibrium model. The maximum

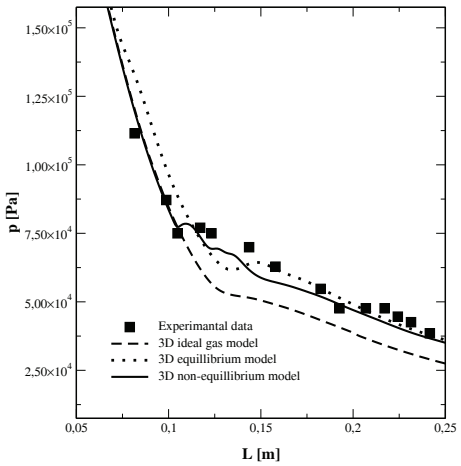

Figure 2. Static pressure drop in de Laval nozzle.

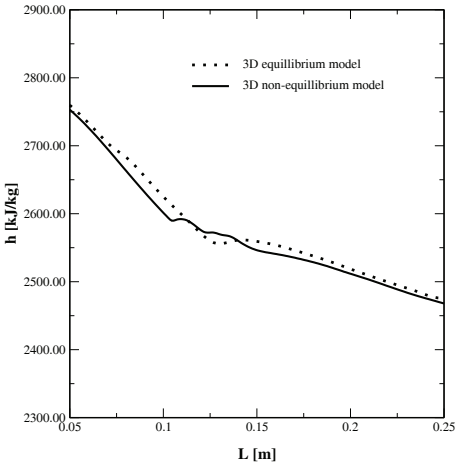

Figure 3. Static enthalpy changes in de Laval nozzle.

value of steam subcooling is equal nearly to 40 °C. The similar results are presented in [14]. In the subcooling region steam is able to expand to lower enthalpy level before the wetness appears which is shown in Fig. 3.

On the other hand, as we know from works by Perycz [21] and Traupel [22] that thermodynamic wetness loss during the droplet formation process occurs because of the fact that if the steam reaches saturation conditions the nucleation does not appear immediately. The steam remains dry and falls into a thermodynamic nonequilibrium state (NE). The reversion to equilibrium conditions is inseparably associated with entropy production ($\Delta s = s1_{NE} - s1_{EQ*}$, Fig. 4).

In Fig. 4 we can see that expansion line in the h-s diagram. It is assumed that the revision to equilibrium conditions ($1_{NE} - 1_{EQ*}$) takes place at constant pressure and that the non-equilibrium isobars and isothermal lines can be extrapolated from the overheated region into the two-phase region. If the condensation is not as fast as the expansion required for maintaining equilibrium conditions, thermodynamic wetness losses are also generated during the growth of droplets. The deviation from the corresponding equilibrium state is characterized by subcooling $\Delta T = T_s - T_g$ [21,22]. However, the non-equilibrium simulation shows subcooling of the steam in the first part of de Laval nozzle (Fig. 5) and condensation primarily takes place at about $L = 0.1$ m. The not yet released latent heat leads to higher enthalpy decrease of the first part of the de Laval nozzle compared to the 3D equilibrium model. The similar results of enthalpy drop comparisons are presented in [10].

When the spontaneous condensation occurs far away from equilibrium conditions, the latent heat is being released and temperature increases suddenly what

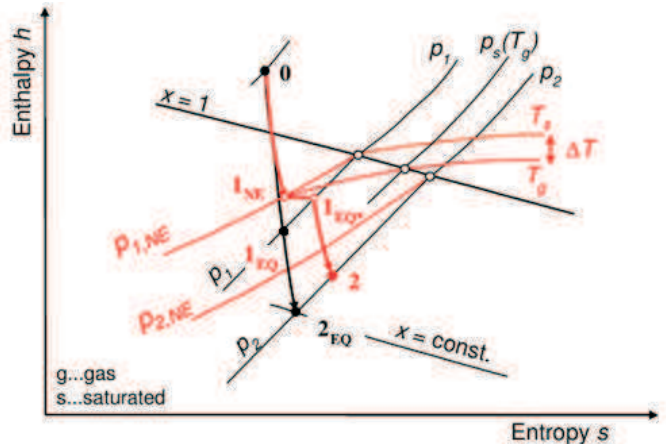

Figure 4. Nonequilibrium and equilibrium expansion presented in the h-s diagram, where: 0,2 – real points of process; $1_{EQ}, 2_{EQ}$ – points of equilibrium process; 1_{NE} – point of nonequilibrium process 1_{EQ*} – point of the revision to equilibrium conditions, T_g – temperature of subcooled vapor, T_s – temperature of saturated vapor [21,22].

is predicted properly by the nonequilibrium model. An equilibrium model is not capable to predict this phenomena. Due to spontaneous condensation process the droplets start to form rapidly and the locally averaged wetness fraction increases dramtically when the nonequilibrium model is employed. On the other hand, the equilibrium model predicts rather slow and linear growth of wetness fraction. However, at the nozzle exit the same level of wetness fraction is estimated by both models and the values are equal to these which are known from measurements [1]. It can be observed in Fig. 6.

4 Numerical analysis of low-pressure part of Baumann steam turbine

4.1 The Baumann stage geometry and numerical modeling

Several papers have already been devoted to the modeling of a condensing flow through the low pressure (LP) part of steam turbine [10, 11, 13]. This issue is especially difficult when the turbine geometry is a complicated one, therefore an enormous number of finite volumes is necessary for domain discretization. One geometrical example is a low-pressure part equipped with the Baumann stage, which is a construction that has been widely employed in the turbines of large output. Full geometry of blades sets, the inlet casing, the outlet exhaust hood are presented in paper [15]. Two paths of steam, i.e., inner and outer, can be distinguished in the last two stages (known as the Baumann stage). Radial clearances

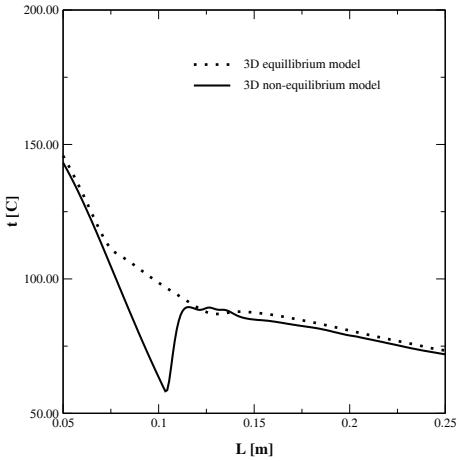

Figure 5. Temperature changes in de Laval nozzle.

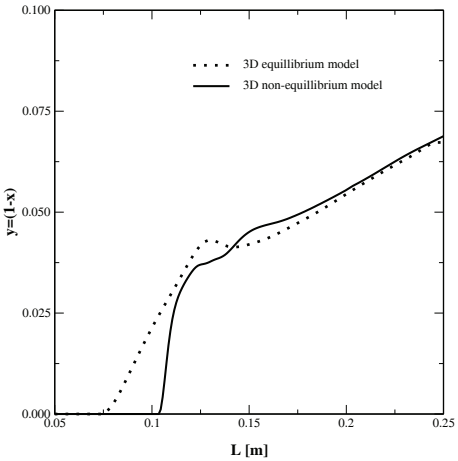

Figure 6. Wetness fraction changes in de Laval nozzle.

between the casings and rotor blades as well as damping wires were taken into account in our geometrical model.

Computations have been performed for the inlet parameters such as mass flow rate $\dot{m} = 65.194$ kg/s and steam temperature $T_{in} = 179.2$ °C. Pressure in condeser was at the value of $p_{out} = 2.3$ kPa. Due to relatively small computational cost of using ideal gas or equilibrium model, full blade sets calculations were performed in those cases. In order to employ the nonquilibrium model, mixing planes have been used in single channel calculations to avoid memory constraints. Both single channel and full blade sets calculations gave the same results. Circumferential pressure at last stages was almost uniform because of splitting sheets existence in the exhaust hood.

4.2 Comparison of the models

Several steam parameters data sets of LP work points were taken off from the Turbina 0D code, which is based on experimental measurements [12]. This data sets are further compared to other steam models. In assumption to the 0D Turbina code [19] calculates wetness directly from pressure and enthalpy so it means to perform an equilibrium approach. The wetness fraction, temperature and average static pressure drop throughout both outer and inner paths are presented in Fig. 7. The 0D prediction and equilibrium condensation model provides the same pressure results, but different wetness level. This can be explained by higher losses obtained in Turbina code as can be seen in Fig. 8. Equilibrium model in both Figs. 8 and 9 overpredicts pressure at entry region while ideal gas model agrees with the nonequilibrium case.

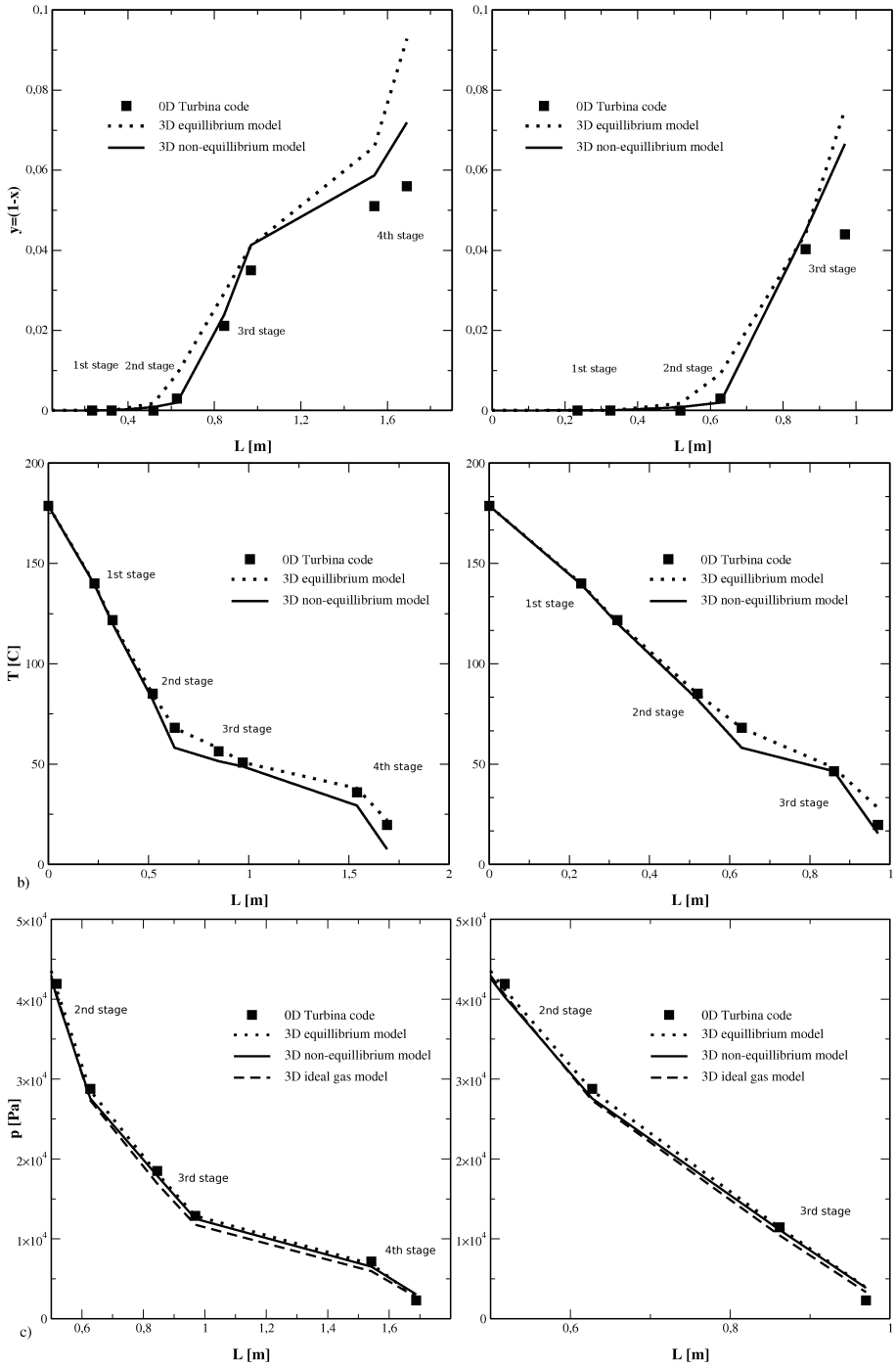

Figure 7. Steam parameteres changes through inner (left side) and outer (right side) channel: a) wetness factor, b) static temperature, c) static pressure.

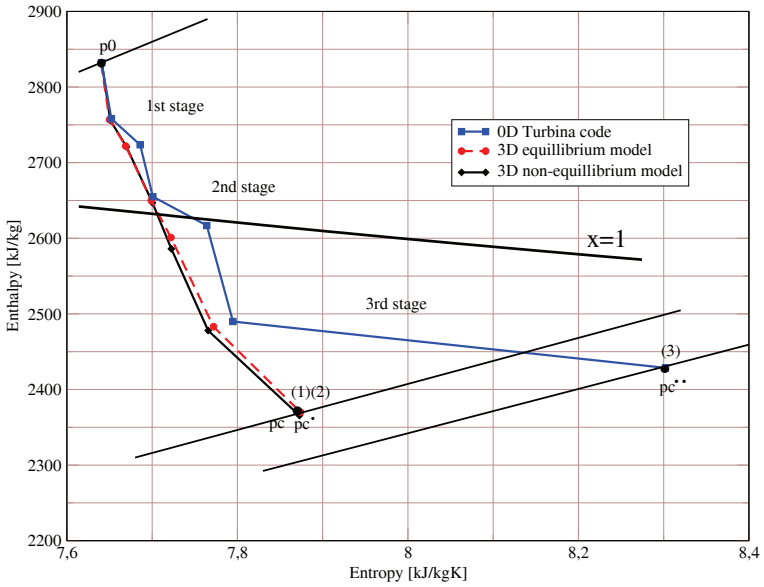

Figure 8. Enthalpy-entropy diagram for outer path of steam turbine LP part.

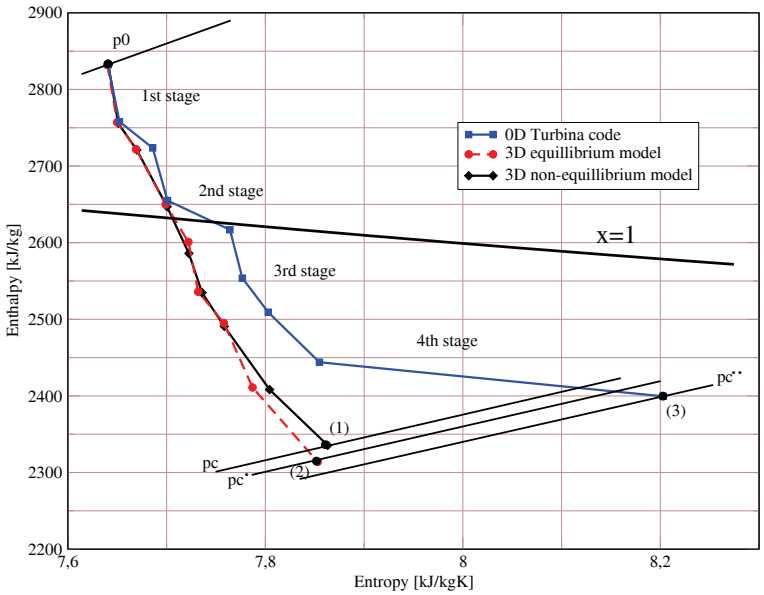

Figure 9. Enthalpy-entropy diagram for inner path of steam turbine LP part.

4.3 Influence of nonequilibrium

As it is reported in the paper by Starzmann *et al.* [10] the mass flow rate difference between nonequilibrium and equilibrium case is lower than 1%, therefore it is ex-

pected that such mass flow rate changes lead to negligible flow velocities changes, but inlet flow angles in condensation region can change up to 5%. It is also expected that the efficiency for nonequilibrium case is lower than for equilibrium case due to the irreversible heat transfer caused by the condenastion process [10].

In the Baumann stage calculations the total power output was approx. 2% higher in equilibrium than in the nonequilibrium approach. However, in the first two stages of steam turbine a lower work output is noticed compared to nonequlibrium model. This can be explained by the existence of subcooling region and ability of steam to expand to lower enthalpy level. The outlet pressure, p_{out}, depends strongly from the condenser temperature which was taken equally to every three models $T_{out} = 37$ °C. Depending on the model, a different supersaturation pressure can be obtained p_c, p'_c, and p''_c. This leads to different points (1), (2), and (3) of steam expansion after the last stages of LP part. From Figs. 7-9 it can be seen that steam expansion calculated with the 0D Turbina code bases on classical approach [21,22], which assumes higher entropy losses are generated on the reversion to equilibrium conditions. Therefore we can see the difference on the expansion line calculated by 3D and 0D approaches (Figs. 8–9). Very low condenser backpressure obtained with an open cooling water system localy generates the shock waves in the area of diffuser.

5 Summary and conclusions

In the paper a homo- and heterogeneous model of nonequilibrium steam condensation internaly coupled with turbulence evolution is presented. It has been shown that su ch a model is dedicated mainly to steam flows throughout the low-pressure parts of turbines of large output. This model possesses a conservative form and therefore should be implementable into CFD codes.

Models of different kinds have been tested and compared with experimental data. It has been found that only the model of nonequilibrium condensation can efficiently predict the flow through the de Laval nozzle that operates in the wet-steam area. Using directly the same model for the full set of blades, as in the case of low-pressure part of steam turbine, is however difficult due to the computer constraints. Results indicate that the basic operational parameters as an average pressure distribution can be efficiently predicted by means of simple equilibrium condensation model. Detailed information can be estimated only by employing a nonequilibrium model. Turbina code assumes that pressure at the last stage is the same as in condenser. This simplification leads to some divergence in results.

Received 23 June 2012

References

[1] Puzyrewski R.: *Theoretical and experimental studies on formation and growth of water drops in LP steam turbines.* Trans. IFFM, **42-44**(1969), 289–303.

[2] Puzyrewski R., Krzeczkowski S.: *Some results of investigations on water-filem break-up and motion of water drops in aerodynamic trail.* Trans. IFFM, **29-31**(1966), 21–44 (in Polish).

[3] Garmathy G.: *Condensation in flowing steam.* In: Two-Phase Steam Flow in Turbines and Separators. (M.J. Moore, C.H. Sieverding, Eds.). Hemisphere Pub., 1976, 127–189.

[4] Krzyżanowski J.: *Erosion of the steam turbine blades.* Maszyny Przepływowe, Vol. 6. Ossolineum, Wrocław 1991 (in Polish).

[5] Badur J., Bilicki Z.: Kwidziński R.: *Operational volumetric viscosity in the process of momentum transport during water expansion and shock steam condensation.* Bull. IFFM PAS 479/1428/1997 (in Polish).

[6] Schnerr H., Badur J.: *Multiphase flows and problems related to the condensation and cavitation processes.* Rep. IFFM PAS 23/2002, 1–44, Gdańsk 2002.

[7] Stastny M., Sejna M., Jonas O.: *Modeling of the flow with condensation and chemical impurities in steam turbine cascades.* In: Proc. 2nd Europ. Conf. Turbomachinery, Antwerpen 1997, 23–29.

[8] Stastny M., Sejna M.: *Numerical analysis of hetero-homogeneous condensation of the steam flowing in turbine cascade.* IMechE **557**(1999), 815–826.

[9] Bilicki Z., Badur J.: *A thermodynamically consistent relaxation model for a turbulent, binary mixture undergoing phase transition.* J. Non-Equilibrium Thermodyn. **28**(2003), 145–172.

[10] Starzmann J., Casey M., Sieverding F.: *Non-equilibrium condensation effects on the flow and the performance of a low pressure steam turbine.* GT2010-22467, In: Proc. of the ASME Turbo Expo 2010: Power for Land, Sea and Air, Glasgow, 14-18 June, 2010.

[11] Gerber A.G., Sigg R., Volker L., Casey M.V., Surken N.: *Predictions of non-equilibrium phase transtion in a model low-pressure steam turbine.* IMechE A: J. Power Energy **221**(2007), 825–835.

[12] Błażko E.: *Modernization concept of low pressure part of turbines PWK-200, TK-200, 13K-215 installed in power stations with an open cooling water system.* Rep. IFFM PAS 41/89, Gdańsk 1989 (in Polish).

[13] Wróblewski W., Dykas S., Gardzilewicz A., Kolovratnik M.: *Numerical and experimental investigations of steam condensation in LP part of a large power turbine*. Trans. ASME J. Fluids Eng. **131**(2009), 041301, 1–11.

[14] Yang Y., Shen S.: *Numerical simulation on non-equilibrium spontaneous condensation in supersonic steam flow*. Int. Commun. Heat Mass Tran. **36**(2009), 902–907.

[15] Karcz M., Zakrzewski W., Lemański M., Badur J.: *Problems related to the modelling of spontaneous condensation in the low-pressure part of 200 MW steam turbine*. In: Proc. of 10th Int. Conf. on Heat Power Plants, Exploitation - Modernization - Remonts, Słok/Bełchatów, 6–8 June, 2011 (in Polish).

[16] Badur J., Karcz M., Lemański M., Zakrzewski W., Jesionek K.: *Remarks on steam condensation modelling related to steam turbine of large output*. In: Proc. of microCAD, Int. Sci. Conf., Miskolc 2011.

[17] Vukalovich M.P.: *Thermodynamic properties of water and steam*, 6 Edn. MASHGIZ Pub., Moscow 1958 (in Russian).

[18] www.ansys.com

[19] Lidke M., Błażko E.: *One dimensional flow code for turbine calculations*. Rep. IFFM PAS 88/78, Gdańsk 1978.

[20] Marcinkowski S.: *Experimental determination of the formation of condensation in the steam turbine of large output*. Teploenergetika **1**(1983), 69–71 (in Rusian).

[21] Perycz S.: *Steam and gas turbine*. Gdańsk University of Technology, Gdańsk 1988 (in Polish).

[22] Traupel W.: *Thermische Turbomaschinen*, 4th Edn. Berlin 2001.